Fouling mitigation of a dead-end microfiltration by mixing-enhanced preoxidation for Fe and Mn removal from groundwater

Jr-Lin Lin [a], Chihpin Huang [a,*], Pan Jill Ruhsing [b], Yau-Shian Wang [a]

[a] Institute of Environmental Engineering, National Chiao Tung University, Hsinchu, Taiwan
[b] Department of Biological Science and Technology, National Chiao Tung University, Hsinchu, Taiwan

HIGHLIGHTS

- ▶ The reduced cake resistance is caused by mixing-enhanced preoxidation.
- ▶ A hydrophobic cake aggravates membrane fouling as Fe–Mn oxides form.
- ▶ The irreversible fouling induced by Fe–Mn oxide is severer than that by Fe oxide.

GRAPHICAL ABSTRACT
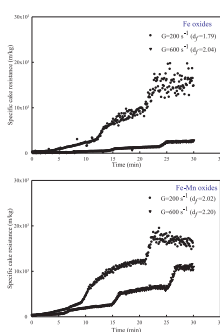
ARTICLE INFO

ABSTRACT

A combination of oxidation and microfiltration (oxidation-MF) is commonly used to remove Fe and Mn from groundwater. The characteristics of Fe and Mn oxides formed by oxidation can be significantly affected by the mixing intensity during oxidation, which subsequently influences the performance of membrane filtration. To optimize oxidation-MF, the critical role of mixing intensity on Fe and Mn oxide formation was investigated. Sufficient oxidant (NaOCl) was added to a prepared ferrous solution with or without Mn ions to oxidize the ions at different mixing intensities, followed by a dead-end MF for 30 min at a constant transmembrane pressure of 1 kg/cm^2. A custom-made module surrounded by a tube membrane was used in microfiltration. The resistance of membrane filtration was calculated by a resistance-in-series model. Cake resistance (R_c) dominated the fouling of the membrane, which depended on the composition of oxides. Oxides formed at high mixing intensity were smaller and more compact, which resulted in reduced R_c and increased permeate flux. The presence of oxidized Mn aggravated membrane fouling. Permeate flux declined rapidly as a result of the cake formed by Fe–Mn oxides with increased hydrophobicity. The irreversible fouling of the dead-end MF was insensitive to mixing intensity during prechlorination, while the irreversible fouling induced by Fe–Mn oxides was more severe than that by Fe oxides as membrane filtration cycle progressed. The results show that membrane flux of a dead-MF can be effectively improved by prechlorination with enhanced mixing due to the formation of a permeable cake layer with low cake compressibility in the membrane filtration.

© 2012 Elsevier B.V. All rights reserved.

1. Introduction

Fe and Mn are found in groundwater in their most soluble form, Fe(II) and Mn(II) ions, and in the oxide form, Fe_2O_3 and MnO_2. Conventionally, raw water is first oxidized, and then filtered to remove the oxide solids. Vigorous oxidation is needed to comply with

* Corresponding author. Tel.: +886 3 5712121x55507; fax: +886 3 5725958.
E-mail address: cphuang@mail.nctu.edu.tw (C. Huang).

discharge regulations. Without oxidation, ferrous and manganese ions can easily escape water treatment processes and continue to oxidize to become insoluble oxides in the distribution system, thus causing water discoloration, metallic taste, odor and turbidity [1]. For these reasons oxidation is an important step in water treatment for Fe and Mn removal.

Oxidation can be achieved by aeration or by the use of oxidants such as chlorine, potassium permanganate, hypochlorite, chlorine dioxide, or ozone. An oxidation–filtration process is commonly used to remove Fe and Mn ions in a conventional water treatment plant. Ideally, oxidants are added first to transform Fe and Mn ions into oxides which can be removed by subsequent filtration. The efficiency of membrane filtration relies on the type and amount of the metal oxides formed in the oxidation stage.

Membrane filtration, both microfiltration (MF) and ultrafiltration (UF), with pre-chlorination has been demonstrated effective in Fe and/or Mn removal from groundwater [2]. However, insufficient oxidation of Fe and Mn ions would increase membrane fouling and reduce permeate flux. Research, however, has shown that severe fouling can occur during filtration if the oxidation of metal ions is incomplete [3]. Another study found that Mn oxide was major foulant on the membrane [4], because that it takes longer to oxidize Mn(II) than Fe(II) [5]. When the residual unoxidized Mn(II) ions pass through the membrane and continue to be oxidized with time, the oxides may block the pores and foul the membrane [6]. Therefore, the oxidation of Fe(II) and Mn(II) ions is extremely important to guarantee the effectiveness of membrane filtration. Other studies also found that the properties of the oxide particles, such as their size and structure, could significantly affect the permeability of filtration membranes [7–9]. Bizi [10] suggested that mixing intensity during coagulation plays a critical role in the size distribution of particles that affects membrane fouling, where the minimum specific cake resistance occurred at the highest cake porosity and the narrowest particle size distribution. Other work has also found that rapid-mixing during coagulation would influence the rate of particle aggregation and the distribution of aggregates [11]. Thus, mixing intensity is a key factor in the removal of Fe and Mn by a pre-oxidation/membrane filtration process. The effect of pre-oxidation conditions on the performance of membrane filtration for Fe and Mn removal has been investigated [12–14], but few have looked into the effect of mixing intensity on the aggregation of oxides and the behavior of aggregates on membrane filtration.

The goal of this study was to evaluate the effect of mixing intensity on the aggregation of Fe and Fe–Mn oxides and the structure and composition of these oxides on membrane fouling. The size and fractal dimension of oxides were determined by a particle sizer with small-angle static laser scattering (SALLS) before each membrane filtration test. The performance of membrane filtration was evaluated by relative flux and mean flux, while the fouling was analyzed by fouling resistance. In addition, the contact angle of the cake was also measured by the sessile drop method, to determine the hydrophobicity of the cake.

2. Material and methods

2.1. Membrane module

The custom-made MF module used in this study is shown in Fig. 1. The single tube polypropylene membrane with an effective surface area of 0.012 m^2 and pore size of 0.7 μm is wrapped around the support, as seen in the top view of the module (Fig. 1(b)). During filtration, the pressure pushes the membrane toward the support. As filtration progresses, a cake layer builds up (Fig. 1(d)). After filtration, the cake on the membrane surface is removed
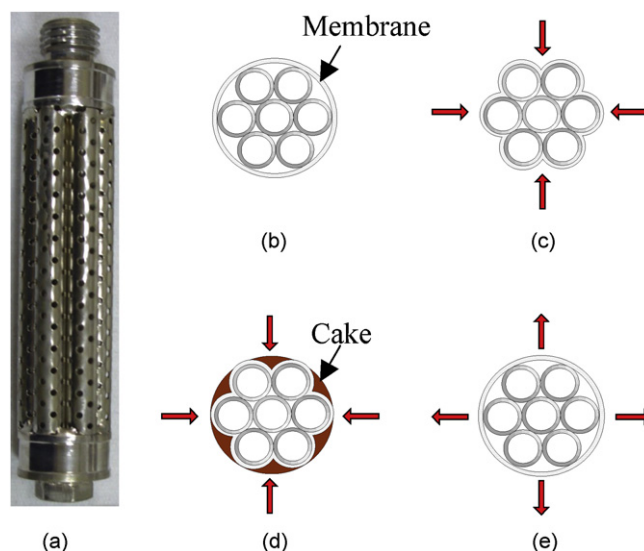

Fig. 1. Illustration of filtration procedure of tube membrane surrounding a custom-made module. (a) Side-view of the module; (b) top-view of the module; (c) filtration; (d) cake formation; (e) air backwashing.

by backwashing with air and water with a constant pressure of 2.5 kg/cm^2, to complete one filtration cycle.

2.2. Chlorination/membrane filtration

The bench-scale MF system with preoxidation is shown in Fig. 2. The system operation and data collected were automated by a programmable logic controller and an on-line computer. The feed water contained 10 mg/L ferrous ions, with/without 3 mg/L manganese ions. Before membrane filtration, a NaOCl solution with 20 mg/L as Cl was injected into the feed solution to oxidize the ions. The injected NaOCl was mixed with the feed water at different velocity gradients (G) (i.e., $G = 200\,s^{-1}$ and $600\,s^{-1}$) for 5 min. The oxides formed from chlorinated ferrous solution are designated Fe oxides, while those from chlorinated ferrous mixed with manganese solution are designated Fe–Mn oxides. The chlorinated feed water was continuously pumped into the dead-end MF unit for 30 min at a constant transmembrane pressure (TMP) of 1 kg/cm^2. To make up the background ions in natural groundwater, CaCl$_2$ and MgCl$_2$ were simultaneously added into the feed water (i.e., 100 mg/L Ca and 20 mg/L Mg). The pH of the chlorinated feed water before membrane filtration was about 8.

The clean-water flux (J_0) of the membrane unit was determined by filtering tap water through the membrane. Each experiment consisted of four filtration cycles, and each cycle consisted of a filtration and an air backwash process at a pressure of 2.5 kg/cm^2. The contact angle of the cake was measured by the sessile drop method, with a contact-angle measuring instrument (Model 100, Sindatek) to determine the hydrophobicity of the cake. The component resistances of membrane filtration were calculated by the resistance-in-series model. The relationship between permeate flux and resistances can be expressed as follows:

$$J = \frac{\Delta P}{\mu R_t} = \frac{\Delta P}{\mu (R_m + R_f + R_c)} \tag{1}$$

where J is the permeate flux, ΔP is the TMP, μ is viscosity of permeate, R_t, R_m, R_c and R_f are total, membrane, cake and fouling resistance, respectively.

R_m, R_f and R_c can be calculated, respectively, as follows:
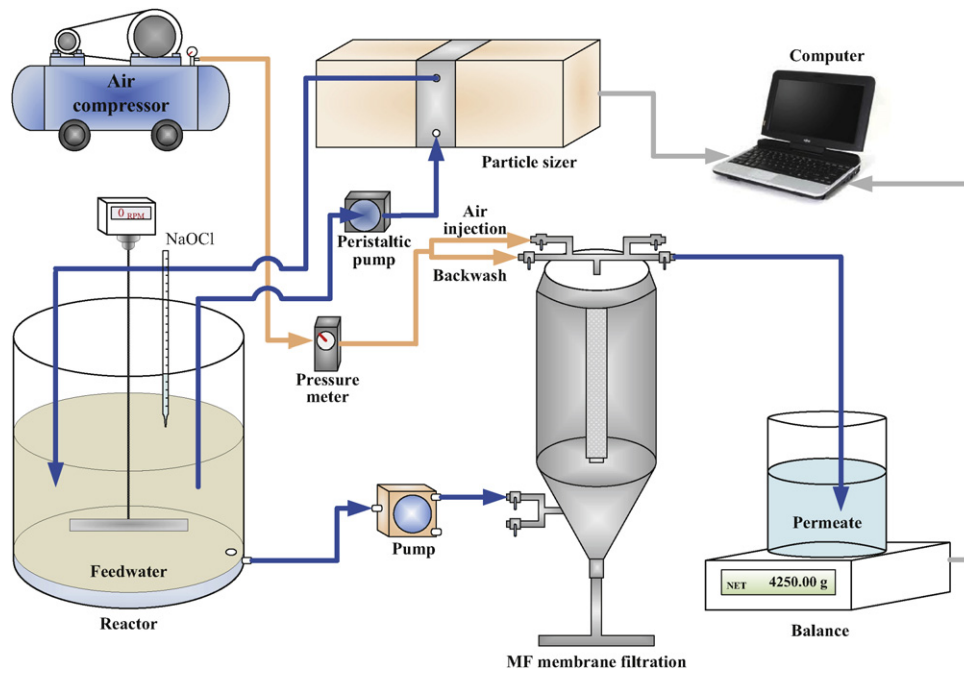
$$R_m = \frac{\Delta P}{\mu J_0} \tag{2}$$

Fig. 2. Schematic diagram of the bench-scale dead-end microfiltration system with prechlorination.

$$R_f = \frac{\Delta P}{\mu J_2} - R_m \qquad (3)$$

$$R_c = \frac{\Delta P}{\mu J_1} - R_m - R_f \qquad (4)$$

where J_0 is clean water flux, J_1 flux of oxidized samples, and J_2 clean water flux after the backwash of the filtered membrane.

Specific cake resistance, α, is related to cake resistance, R_c, and the mass of cake deposited on the membrane surface, M, can be shown as follows:

$$R_c = \frac{\alpha \times M}{A_m} = \frac{\alpha V C_b}{A_m} \qquad (5)$$

where A_m is the membrane area, V is the cumulative permeate volume, and C_b is the bulk concentration of particles.

2.3. Size and structure of oxidized particles

A particle size analyzer (Mastersizer 2000, Malvern, UK) with a small angle static light scattering (SASLS) was used to monitor the dynamics of oxides growth during chlorination and the structure of aggregates. During chlorination, the suspension was pumped to the SASLS by a peristaltic pump (EW-7553-70, Cole-Parmer Instrument Co., USA) with a Tygon tubing (Masterflex-06409-16, Cole-Parmer Instrument Co., USA) of I.D. 3.1 mm, and the sample was recycled back to the mixing vessel at a flow rate of 20 mL/min. The size of oxides formed at a constant mixing intensity was continuously measured for 30 min by use of the particle size analyzer, and fractal dimensions of those oxides were determined by SALLS [15].

2.4. Foulants on the membrane

An FE-SEM (JSM-6330F, JEOL, Japan) coupled with an X-ray energy-dispersive spectrometer (EDS) detector was used for imaging and characterization of the Fe and Fe–Mn oxides within the membrane at acceleration voltages of 15 and 10 kV, respectively. After the last filtration cycle, the backwashed membrane was air dried before SEM scanning.

3. Results and discussion

3.1. Effect of mixing intensity on oxides aggregation

The incomplete oxidation of Fe and Mn ions before filtration could accelerate membrane fouling and reduce the efficiency of Fe and Mn removal [6]. To oxidize Fe and Mn ions completely before membrane filtration, sufficient chlorination time must be provided. After the NaOCl was added, the feed water was mixed for one or two minutes at various mixing intensity to complete oxidation, and then the chlorinated water was immediately pumped to the filtration unit. The residual ion concentration in the permeate was determined when mixing was stopped. As shown in Fig. 3, little residual Fe and Mn remained after 2 min oxidation, confirming that the majority of Fe and Mn ions can be effectively oxidized by chlorination in 2 min and then removed by membrane filtration, similar to the findings of other studies [16].
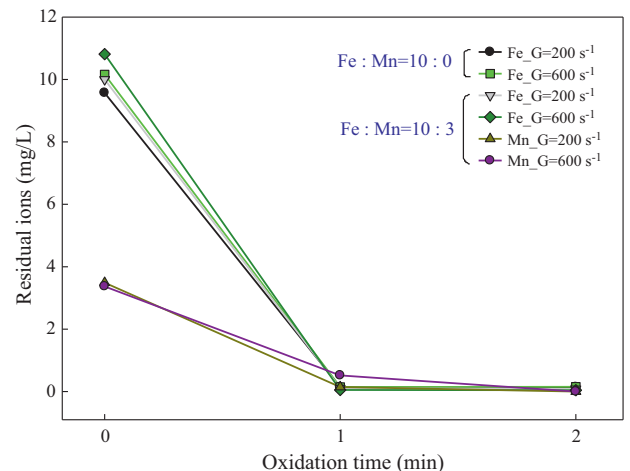

Fig. 3. Residual dissolved Fe and Mn after chlorination-filtration process at different oxidation times and different mixing intensities.
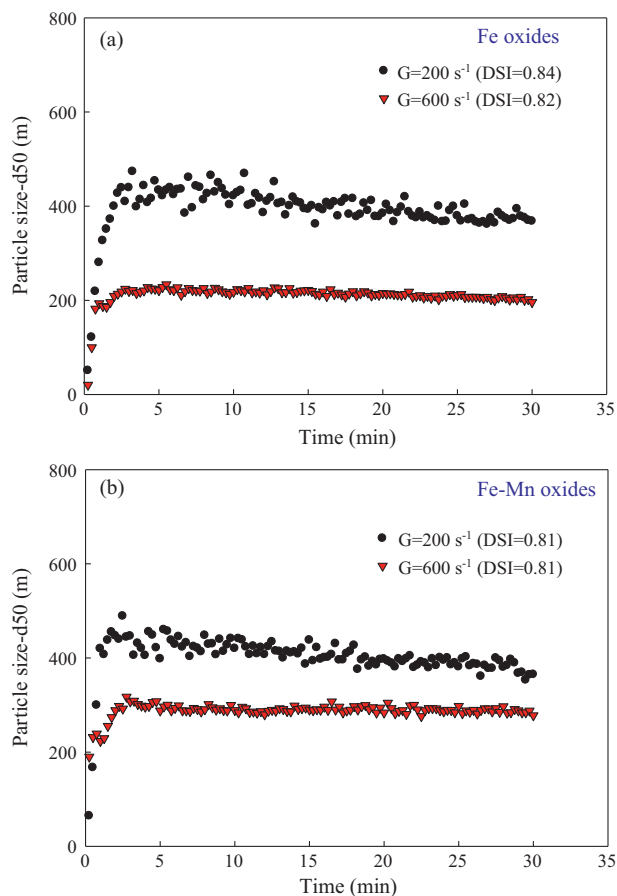
Fig. 4. Variation in the d_{50} size of Fe and Fe−Mn oxides with mixing time during chlorination at different mixing intensities. The distribution spreading index (DSI) is expressed by $(d_{90} − d_{10})/2(d_{50})$. d_{90}: diameter corresponding to 90% of cumulative undersize; d_{10}: diameter corresponding to 10% of cumulative undersize; d_{50}: median diameter.

Fig. 5. Decline in relative flux of microfiltration at different mixing intensity for prechlorination.

Other investigations have also suggested that mixing intensity affects the aggregation rate of particles and the structure of aggregates [10,11]. To investigate the effect of mixing on oxide aggregation during chlorination, the profile of oxides aggregation was monitored. Before membrane filtration, chlorination at different mixing intensities was conducted to monitor the growth of oxides and determine the size distribution of aggregates by using a particle size analyzer. Initially, both oxides aggregate to form larger particles, but stopped growing in 5-min mixing (see Fig. 4). Higher mixing intensities were also observed to produce smaller aggregates ($G = 600 s^{-1}$). Previous studies have suggested that the reduced size of aggregates at higher G is caused by the breakage of aggregates by intensive mixing [17,18], and that particle size distribution can influence the porosity of cake layer on membrane [10]. Greater cake porosity will allow fluid to pass through the membrane, which increases permeate flux [19]. To determine the particle size distribution of oxide aggregates, the distribution spreading index (DSI) was further analyzed. Higher DSI values indicate a broader size distribution of particles [10]. At low and high mixing intensities, our DSI values of oxides ranged from 0.81 to 0.84, suggesting a limited difference in particle size distribution between Fe and Fe–Mn oxides. The results of size measurement confirmed that chlorination with enhanced mixing resulted in smaller oxides aggregate, which influences the permeate flux of dead-end MF. Furthermore, the five-minute mixing in chlorination was sufficient for oxide removal by membrane filtration.
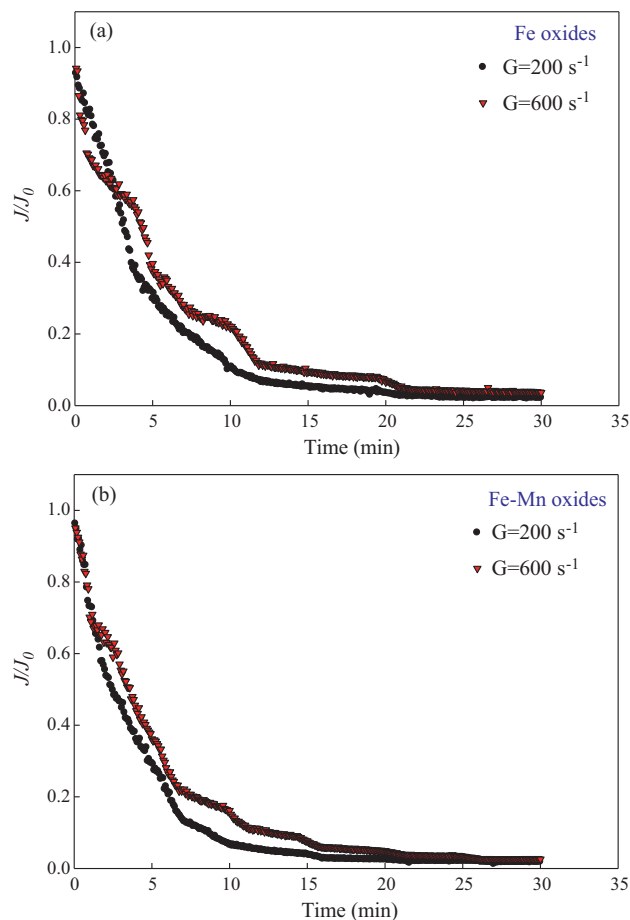
3.2. Effect of mixing intensity on permeate flux

To further verify the significance of enhanced mixing for improved permeate flux in chlorination-microfiltration, the five-minute chlorination with low and high mixing intensities was carried out before each filtration. The relative flux (J/J_0) of the MF membrane with prechlorination at low and high mixing intensities is shown in Fig. 5. A marked difference in flux decline between low and high mixing intensities was observed. A mixing intensity of $600 s^{-1}$ delayed flux decline substantially for the filtration, and could have been due to the characteristics of the cake layer as suggested by previous study that cake layer formation determines the magnitude of irreversible fouling [20]. Other researchers have also found that cake porosities are affected by the properties of aggregates such as size and fractal dimension [21]. As a result, mixing intensity during chlorination can significantly affect the properties of cake layer formed by Fe and Fe–Mn oxides in microfiltration. Furthermore, the magnitude of flux decline of membrane filtration with Fe oxides is less than that with Fe–Mn oxides at a constant mixing intensity during chlorination. This suggests that the composition of oxides influences the properties of a cake layer in addition to mixing intensity. The results show that permeate flux of membrane filtration can be effectively improved by enhanced mixing for Fe and Mn oxidation for 5 min. It was also found that the presence of Mn aggravates the membrane fouling. The characteristics of the oxides can also determine the subsequent cake layer on membrane surfaces. In other words, the oxides formed from chlorination could indirectly influence the performance of membrane filtration.

Table 1
Membrane filtration resistance of oxide suspensions formed at low and high mixing intensities with filtration pressure of 1 kg/cm^2 over 4 cycles.

Velocity gradient (G)	Membrane filtration resistance					
	Fe oxides			Fe–Mn oxides		
	R_m (%)	R_f (%)	R_c (%)	R_m (%)	R_f (%)	R_c (%)
200 s^{-1}	2–17	16–17	66–82	2–17	20–25	63–74
600 s^{-1}	2–28	17–23	49–81	2–18	19–22	63–77

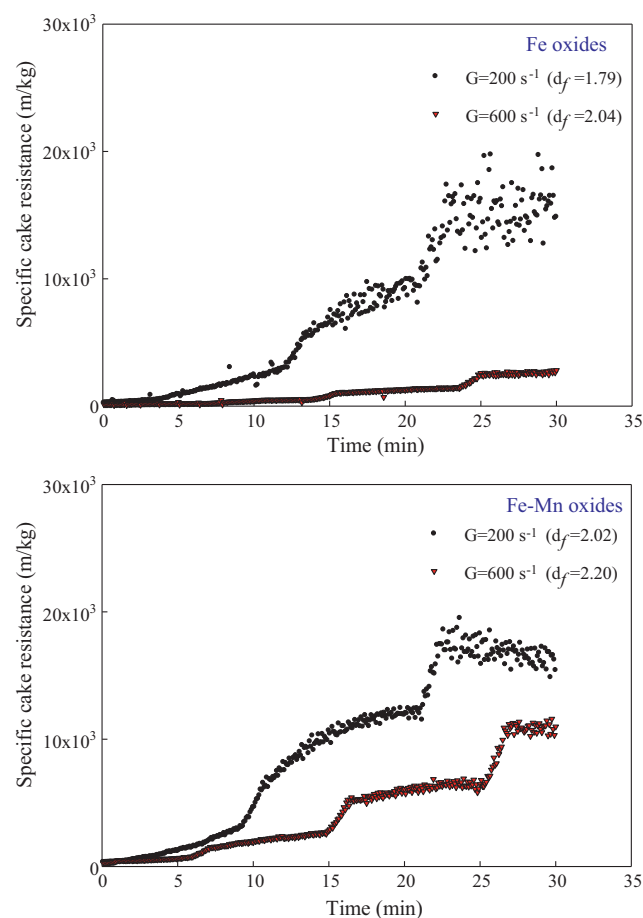### 3.3. Effect of cake properties on membrane permeability

Component membrane resistances (i.e., R_f, R_c and R_t) were calculated by Eq. (1) of the resistance-in-series model to examine the effect of mixing intensity on aggregates, and the resulting cake property on membrane permeability. The resistances over 4 filtration cycles are summarized in Table 1. Cake resistance (R_c) is generally the primary resistance in membrane filtration. Most membrane resistance is the result of cake resistance, R_c: the properties of a cake layer thus play a critical role in cake permeability. Other work has suggested that during filtration, cakes containing high cake compressibility lead to low cake porosity and high specific cake resistance [22], which reduces the cake permeability. Aggregates with a high fractal dimension (d_f) can resist the collapse of cakes, which lowers cake compressibility [21,23]. A previous study of ours found that cake compressibility was mainly governed by the structure of aggregates formed prior to membrane filtration [9]. Other studies have suggested that the cake layer formed from aggregates with high d_f has low specific cake resistance [7,8], which results in increased permeate flux. Fig. 6 shows the variation of specific cake resistance with filtration time at low and high mixing intensities during chlorination. At low mixing intensity, the cake layer of both oxides exhibited much higher specific cake resistance, along with smaller d_f, which accelerates the decline of the relative flux, as seen in Fig. 5. The results show that flux can be improved by enhanced-mixing oxidation as a result of the formation of a permeable cake layer with low cake compressibility in the membrane filtration.

However, the cake layer formed by oxides with lower d_f can worsen the performance of membrane filtration because of increased specific cake resistance. In this study, the d_f of Fe–Mn oxides formed at a constant mixing intensity is greater than that of Fe oxides. But, permeate flux is reduced by the formation of Fe–Mn oxides at a constant mixing intensity, as illustrated in Fig. 5. Cake permeability can thus be affected by the composition of oxides. In/during the oxidation of Fe and Mn, a bulk/prevalence of Fe–Mn oxides can easily be formed in the presence of Mn oxides [14]. As a result, the surface roughness of cake layers formed by Fe and Fe–Mn oxides differs, resulting in varied cake permeability. To verify this, the contact angle of the cake surface on a fouled membrane was determined. The contact angle of the cake layer formed with Fe–Mn oxides is greater than that with Fe oxides at a fixed mixing intensity, as shown in Table 2, indicating that Fe–Mn oxides are more hydrophobic than Fe oxides. Surfaces with increased hydrophobicity have greater roughness than less hydrophobic surfaces [24,25]. It is likely that the smaller Mn oxides adsorb on the surface of Fe

Fig. 6. Variation in specific cake resistance with filtration time at different mixing intensities in a chlorination–microfiltration process.

oxides and enhance the roughness of the cake, resulting in a surface with higher hydrophobility. This process could also worsen the performance of membrane filtration, and as a result, the mean permeate flux of dead-MF membrane in the filtration of Fe–Mn oxides significantly declines.

3.4. Effect of Fe and Fe–Mn oxides on irreversible fouling

Although fouling resistance (R_f) is not the major resistance of dead-end MF, as shown in Table 1, it has a significant effect on permeate flux and backwashing in a long-term filtration process. To understand the magnitude of irreversible fouling accumulated by component oxides during dead-end MF, the mean permeate flux of MF after prechlorination with low and high mixing intensity in four filtration cycles was determined, and as illustrated in Fig. 7, the mean permeate flux was improved by increased mixing intensity. In the first cycle, the mean permeate flux of the suspension of Fe–Mn oxides was less than that of Fe oxides. However, with further filtration cycles, the decline in mean permeate flux became severe. No difference was observed at the fourth cycle, which could
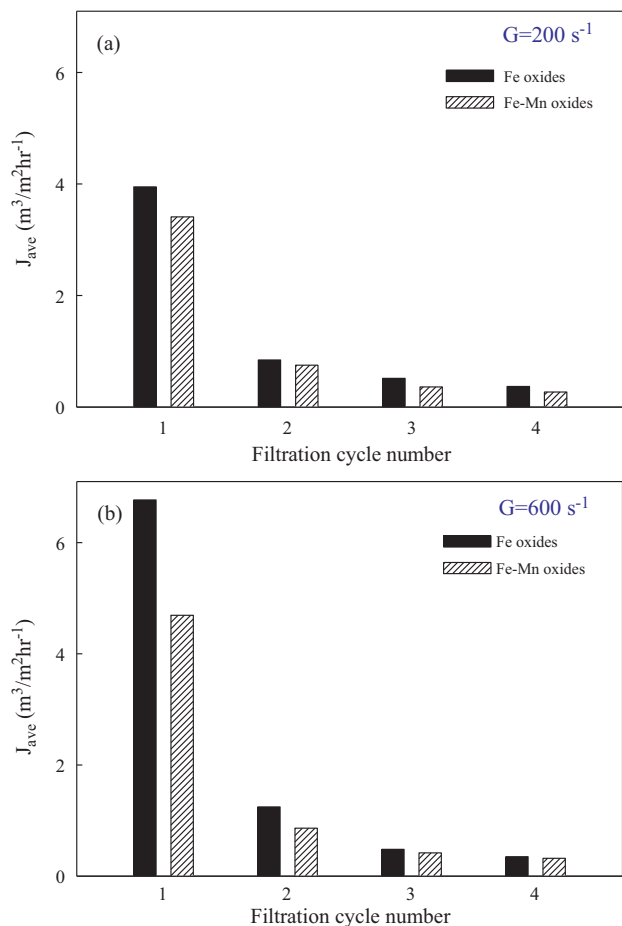
Table 2
Contact angle of cake layer formed from Fe and Fe–Mn oxides after chlorination with low and high mixing intensities.

Velocity gradient (G)	Contact angle (°)	
	Fe oxides	Fe–Mn oxides
200 s^{-1}	77.67 ± 0.41	92.9 ± 0.85
600 s^{-1}	85.07 ± 1.16	109.07 ± 2.68

Fig. 7. Variation in mean flux of progressive filtration cycle of the dead-end micro-filtration at different mixing intensities for prechlorination.
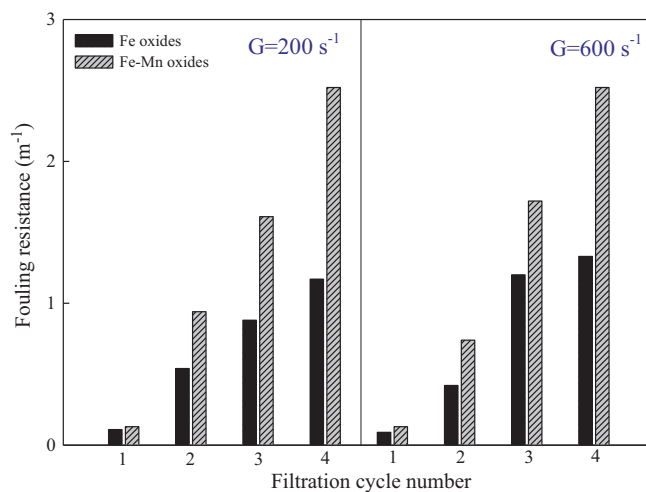

Fig. 8. Variation in membrane fouling resistances of progressive filtration cycle of the dead-end microfiltration at different mixing intensities for prechlorination.

be attributed to irreversible fouling that occurred during filtration and backwashing cycles.

The fouling resistances (R_f) of Fe and Fe–Mn oxides formed at low and high mixing intensities are shown in Fig. 8. The R_f increased with progressing filtration cycles as a result of increased pore plugging within the membrane after filtration, even though backwashing had been carried out. With each additional filtration cycle, the R_f for Fe/Mn-oxide layer became much more severe than that for Fe-oxide layer. Other work has suggested that the formation of Mn oxides within membrane pores causes major irreversible fouling during membrane filtration [for recycling Fe–Mn oxides] [6]. As shown in the SEM images in Fig. 9, after four membrane filtration cycles pore plugging or narrowing caused by Fe–Mn oxides is more severe than that by only Fe oxides. Moreover, the ratio of Fe
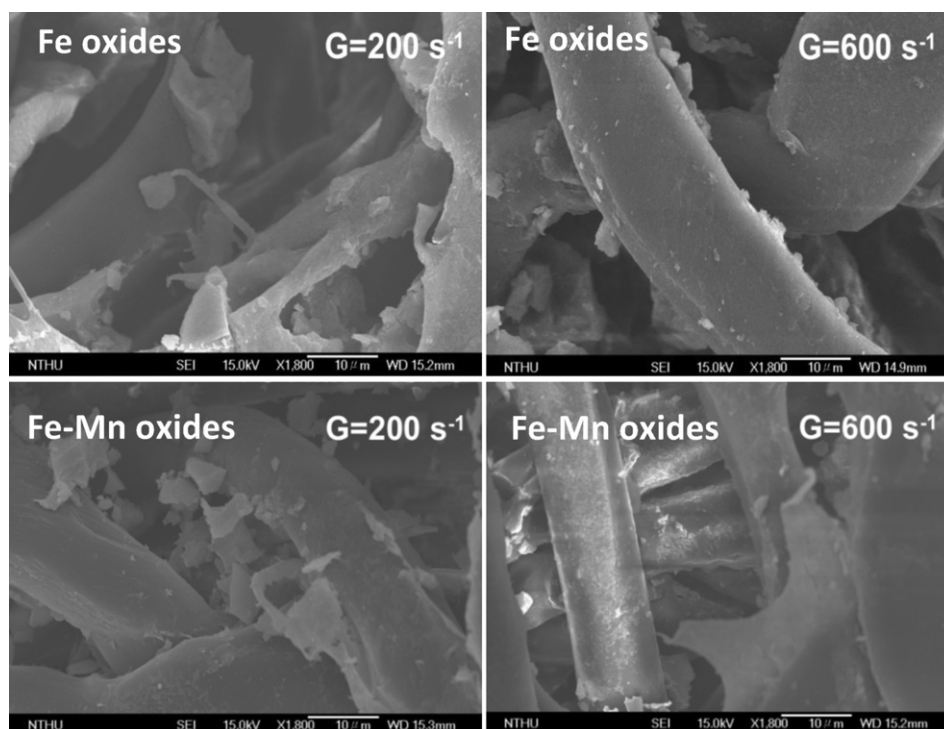

Fig. 9. SEM image of pore clogged membranes after four filtration cycles of the dead-end microfiltration at different mixing intensities for prechlorination.

and Mn oxides within the membrane determined by EDS is approximately 10:3, suggesting that R_f would increase when Mn oxides were completely formed and plugged within membrane. However, the R_f of membrane filtration with Fe or Fe–Mn oxides is insensitive to mixing intensity during/with chlorination in each filtration cycle. Although the oxides formed at high mixing intensity are smaller than those formed at low mixing intensity, most of Fe and Fe–Mn oxides particles formed at low and high mixing intensities during prechlorination are larger than the size of MF membrane pores. As a result, only a few small oxide particles would penetrate the pore of membrane during filtration, resulting in limited difference in R_f for the membrane filtration by low and high mixing-intensity. These results show that the magnitude of irreversible fouling during microfiltration for Fe/Mn-oxide suspensions increases more rapidly than that for Fe-oxide suspensions with increasing filtration cycle regardless of mixing intensity during chlorination.

4. Conclusions

Oxidation with enhanced mixing can improve the performance of membrane filtration in a hybrid chlorination-MF process for the removal of Fe and Mn from groundwater. With increased mixing intensity, cake resistance in membrane filtration is reduced because of the formation of smaller oxide particles with higher fractal dimension, resulting in higher permeate flux. In the presence of Mn ions, the Fe/Mn oxide cake layer formed is more hydrophobic, and more likely to foul the membrane. The irreversible fouling of the dead-end MF by the oxides is insensitive to mixing intensity during prechlorination. To effectively mitigate membrane fouling of the prechlorination/MF process, intensive mixing during prechlorination may be a solution because it promotes the formation of a permeable cake layer rather than lower irreversible fouling during filtration.

Acknowledgement

References

[1] E.D. Breland, L.R. Robinson, Iron and manganese removal from low alkalinity groundwaters, Report to the Water Resources Research Institute, Mississippi State University, MS (1967).
[2] D. Ellis, C. Bouchard, G. Lantagne, Removal of iron and manganese from groundwater by oxidation and microfiltration, Desalination 130 (2000) 255–264.
[3] K.H. Choo, H. Lee, S.J. Choi, Iron and manganese removal and membrane fouling during UF in conjunction with prechlorination for drinking water treatment, J. Membrane Sci. 267 (2005) 18–26.
[4] Y. Kaiya, Y. Itoh, K. Fujita, S. Takizawa, Study on fouling materials in the membrane treatment process for potable water, Desalination 106 (1996) 71–77.
[5] P.C. Singer, D.A. Reckhow, in: Water Quality and Treatment, 4th ed., AWWA, McGraw-Hill Inc, 1990, Chapter 12.
[6] H. Yamamura, S. Chae, K. Kimura, Y. Watanabe, Transition in fouling mechanism in microfiltration of a surface water, Water Res. 41 (2007) 3812–3822.
[7] J. Guan, R. Amal, T.D. Waite, Effect of aggregate size and structure on specific cake resistance of biosolids filter cakes, Water Sci. Technol. 44 (2001) 215–220.
[8] S.A. Lee, A.G. Fane, R. Amal, T.D. Waite, Impact of natural organic matter on floc size and structure effects in membrane filtration, Environ. Sci. Technol. 39 (2005) 6477–6486.
[9] C.P. Huang, J.L. Lin, W.S. Lee, J.R. Pan, B.Q. Zhao, Effect of coagulation mechanism on membrane permeability in coagulation-assisted microfiltration for spent filter backwash water recycling, Colloids Surf., A 378 (2011) 72–78.
[10] M. Bizi, Filtration characteristics of mineral mud with regard to turbulent shearing, J. Membrane Sci. 320 (2008) 533–540.
[11] K. Ebie, T. Kawaguchi, D. Yamaguchi, Dynamic analysis of coagulation of low turbidity water sources using Al- and Fe-based coagulants, Water Sci. Technol. 53 (2006) 67–74.
[12] P. Roccaro, C. Barone, G. Mancini, F.G.A. Vagliasindi, Removal of manganese from water supplies intended for human consumption: a case study, Desalination 210 (2007) 205–214.
[13] M.A. Rahman, J.Y. Huang, Y. Iwakami, K. Fujita, Pursuing the effect of aeration, pH increment, and H_2O_2 coupled with UV irradiation on the removal efficiency of manganese by microfilter membrane, Water Sci. Technol. 41 (10–11) (2000) 25–31.
[14] Z. Teng, J.Y. Huang, K. Fujita, T. Satoshi, Manganese removal by hollow fiber micro-filter. Membrane separation for drinking water, Desalination 139 (2001) 411–418.
[15] J.L. Lin, C.P. Huang, C.J.M. Chin, J.R. Pan, Coagulation dynamics of fractal flocs induced by enmeshment and electrostatic patch mechanisms, Water Res. 42 (17) (2008) 4457–4466.
[16] Y. Jimbo, K. Goto, Iron and manganese removal by a membrane filtration system, Water Sci. Technol. Water Supply 1 (5/6) (2001) 357–364.
[17] P.T. Spicer, S.E. Pratsinis, Shear induced flocculation: the evolution of floc structure and the shape of size distribution at steady state, Water Res. 30 (1996) 1048–1056.
[18] T. Serra, X. Casamitjana, Effect of the shear and volume fraction on the aggregation and breakup of particles, AIChE J. 44 (1998) 1724–1730.
[19] W.L. McCabe, J.C. Smith, P. Harriot, in: Unit Operations of Chemical Engineering, seventh ed., McGraw-Hill, New York, 2005, pp. 163-165.
[20] S.J. Judd, P. Hills, Optimisation of combined coagulation and microfiltration for water treatment, Water Res. 35 (2001) 2895–2904.
[21] P.K. Park, C.H. Lee, S. Lee, Permeability of collapsed cakes formed by deposition of fractal aggregates upon membrane filtration, Environ. Sci. Technol. 40 (2006) 2699–2705.
[22] J.D. Lee, S.H. Lee, M.H. Jo, P.K. Park, C.H. Lee, J.W. Kwak, Effect of coagulation conditions on membrane filtration characteristics in coagulation-microfiltration process for water treatment, Environ. Sci. Technol. 34 (2000) 3780–3788.
[23] B.Q. Zhao, D.S. Wang, T. Li, C.W.K. Chow, C.P. Huang, Influence of floc structure on coagulation-microfiltration performance: Effect of Al speciation characteristics of PACls, Sep. Purif. Technol. 72 (1) (2010) 22–27.
[24] E.M.V. Hoek, S. Bhattacharjee, M. Elimelech, Effect of membrane surface roughness on colloid–membrane DLVO interactions, Langmuir 19 (2003) 4836–4847.
[25] F. Rupp, L. Scheideler, J. Geis-Gerstorfer, Effect of heterogenic surfaces on contact angle hysteresis: dynamic contact angle analysis in material sciences, Chem. Eng. Technol. 25 (2002) 9–15.